Snow Pressure on a Semiflexible Retaining Structure

Snow Pressure on a Semiflexible Retaining Structure

Monica Barbero, Fabrizio Barpi, Mauro Borri-Brunetto
Valerio De Biagi, Gianmarco Olivero, Oronzo Pallara

Department of Structural, Geotechnical and Building Eng., Politecnico di Torino, Italy

Abstract

Snow avalanche hazard is one of the most binding aspects in the urbanization of mountainous areas. The risk due to these natural phenomena can be reduced if proper countermeasures for reducing the danger or preventing avalanche triggering are taken. For instance, in the avalanche initiation zone, devices able to withstand snowpack gliding and to prevent crack propagation can be installed. These can be classified as rigid (snow bridges) or flexible (snow net) structures, depending on the mechanisms involved under snow loading. In recent years, a new kind of structure called a snow umbrella, based on a net panel supported by rigid beams, has been designed and installed in the northwestern Italian Alps. Since the real behavior of these structures is far from being simple to understand because the complex interaction with snowpack movements, an umbrella was instrumented and monitored during the winter season 2010/2011. The recorded data are used for testing two possible pressure distributions and to evaluate the magnitude of the forces acting on the structure. Furthermore, a back-analysis allows validation of the assumptions taken during the design of the devices. The results are compared with commonly used guidelines and further suggestions are proposed.

Keywords: Retaining devices, Snow umbrella, Back-analysis

1 Introduction

Snow avalanches represent one of the most significant natural hazards in mountain areas during winter. These phenomena sometimes make an impact on urbanized areas and, thus, a great deal of effort is spent in order to prevent and mitigate this risk for the population and for the infrastructure. It is very difficult to delocalize important infrastructure, e.g. roads or power lines, because of the topographical constraints in mountainous environments. Thus, alternative solutions have been found to reduce harm to human life and to maintain the serviceability of the infrastructure. In brief, the risk induced by snow avalanches can be mitigated by either reducing the vulnerability of the population or by reducing the incidence of snow avalanche hazards, or both [2]. The former can be achieved by strengthening construction, the latter amounts to reducing the probability of snow avalanche release, e.g. by anchoring the snowpack in initiation zones by natural or artificial means [14].

In this sense, snow retaining structures are conceived and designed in such a way (i) to withstand the thrust of snow, which naturally creeps and slides, and (ii) to limit the extent of shear crack propagation in the snowpack [5]. The formation of cracks, in the majority of cases, leads to the formation of a slab avalanche [6]. Historically, the idea of preventing avalanche triggering was implemented by installing fixed and rigid structures on the mountainside. Snow bridges and snow rakes [5] consisted of steel and/or wood frames with crossbeams parallel or normal to the ground. Since the topography is not always suitable for rigid structures, snow nets made of steel wire were more and more preferred for their capacity to adapt to a wider range of topographical conditions [11]. The development of these kinds of flexible structures was initially proposed by Haefeli [4] and has been further studied by Nicot [8, 7]. The analysis of fifty years of research led to the publication

of the Swiss Guideline [5], which represents the *de facto* international standard for design and site-specific implementation of flexible snow supporting structures for avalanche defense.

In recent years, a new kind of snow retaining structure has been conceived and installed. It can be considered as a semi-flexible device composed of a rigid frame and a flexible net. Since the design of such structures was based mainly on empirical considerations, an experimental assessment of the limit capacity of the device was carried out by Peila et al. [10]. In order to answer questions on the behavior of the barrier onsite, under snow loads, a detailed experimental analysis on an instrumented structure has been conducted. The instrumented snow retaining element, as illustrated in detail in the following, is part of a larger test site designed to study the avalanche movement and its effect on structures.

2 The snow umbrella

The snow umbrella is classified as an active-type defense structure, whose duty is to prevent the triggering of avalanches, arresting the movements of the snowpack at the very beginning, when dynamic effects are negligible.

The umbrella is a lightweight steel structure, designed to optimizeits transport by helicopter and ease of the installation onsite [12]. Its main parts are (Fig. 1):

(a) foundation, consisting of a steel cable inserted in a stabilizing steel tube grouted in a sub-horizontal borehole;

(b) steel anchor plates linking the structure to the foundation;

(c) central steel rod, with circular tubular section (4.2 m long with external diameter equal to 114 mm);

(d) transversal cross, made of 2 HE 120 B steel beams ($L = 4.75$ m);

(e) upslope cables;

(f) feet;

(g) net panel, made of two superposed wire meshes with coarse and fine spacing (3.1 m width, 3.6 m height).

The beams are rigidly connected to one another in the central section; four steel cables connect each beam to a short central strut on the downslope side. A perimeter cable connects the terminal ends of the cross beams, acting as a stiffener and forming, together with the beams, a support for the net panel. This assemblage is linked to the central rod by means of a spherical hinge, which allows the relative rotation between the cross and the central rod. Four cables connect the upslope side of the structure to the anchor plates, maintaining the allowed rotation within the design values. Frontal and lateral schematic views of the snow umbrella are represented in Fig. 2.

The net panel, whose function is to minimize the movement of the snowpack and to transfer its pressure to the other structural elements, is the containing element of the snow umbrella. The panel is built by superposing two orders of meshing: a first-order net of 8 mm diameter twisted steel cables with a grid spacing of 0.3 m, linked to the perimeter cable, and a second-order hexagonal mesh of wires with 3 mm diameter (resulting in a grid spacing of approximately 10 cm).

The structure is pre-assembled off-site and lifted by helicopter to its final position, where it is anchored to the foundation. The umbrellas are arranged side by side in arrays following the altimetric contour lines, with a center to center distance of about 4 m, and with distance along the slope dependent on the site conditions.

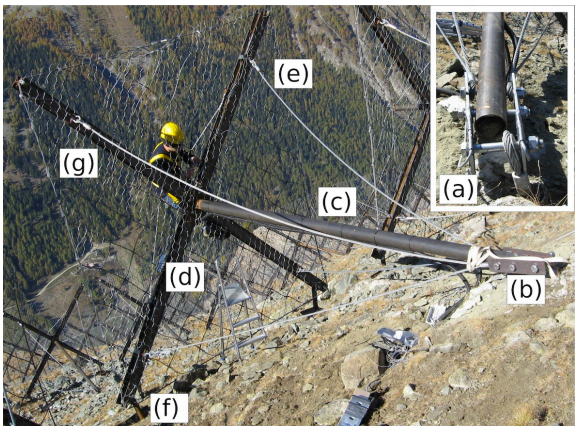

Figure 1: Main parts of the snow umbrella identified on a photograph taken during its installation, photo Borri-Brunetto.

3 The experimental setup

3.1 General

The site chosen for the installation of an instrumented structure for continuous monitoring of the effects of the snow pressure is a slope located at Localité-La-Tour (Valsavarenche, Aosta Valley, Italy), within the Gran Paradiso National Park. Following the large avalanche that struck the village of Les Thoules [1] on December 15, 2008, an active-defence system was installed on the overhanging slope at an elevation between 2325 m and 2575 m a.s.l. comprising 714 snow umbrellas. The instrumented structure has been chosen to represent the average working conditions of a generic element of the array.

The ground, in the neighborhood of the instrumented umbrella has a west aspect and a slope between 29° and 34°; the surface is a thin vegetation cover, mixed with rock blocks of various size (Fig. 3).

The instrumented device is a part of a larger experimental site devoted to the study of snow gliding and its effects on structures. Further details will appear in a specific paper in preparation.

3.2 Instrumentation

The main goals of the research described here were (i) the estimation of the pressure exerted by the snowpack on an umbrella throughout the winter season, and (ii) the estimation, through measurements, of the internal forces in the structure for assessing the correctness of the design assumptions. In order to attain these objectives, the instrumentation setup of the umbrella has been designed to perform the following tasks:

i. measurement of the longitudinal strain at selected sections of one of the cross arms, with the purpose of relating the local deformation to the transversal load on the beams;

ii. measurement of the strain in the anchor plates, to evaluate the total load applied to the structure.

The strain transducers, the control and acquisition system and the data logger have been selected considering the environmental constraints at the installation site. The most important factors that

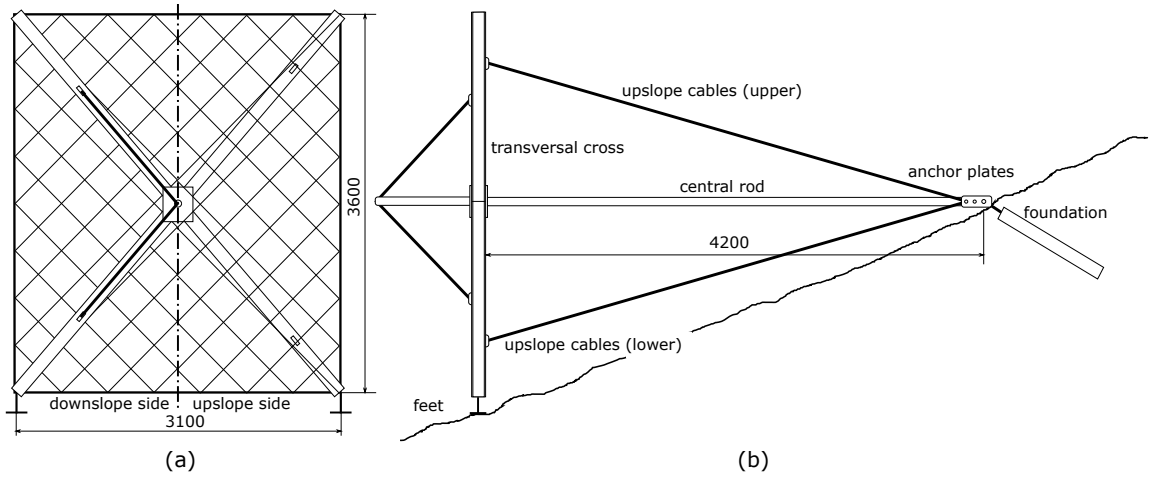

Figure 2: Views of the snow-umbrella. The frontal view (a) represents both the upslope and the downslope sides of the net panel and of the supporting steel structure. The lateral view (b) shows schematically the different components of the snow umbrella. Dimensions are in millimeters.

Figure 3: Arrays of snow umbrellas at the experimental site of Localité-La-Tour, Valsavarenche, photo De Biagi.

influenced the choice were the low-temperature conditions, the scarcity of electric power, the ease of installation, and the mechanical protection of the instrumentation. Because of the impossibility both to visit the site during winter and to remotely transmit the acquired data, the whole system had to work unattended for about six months, storing the measurements on internal memory until the retrieval of the data logger.

The electric power needed to operate the acquisition system is supplied by a photovoltaic panel already in place, used for radio communication by the park authority, located at a distance of about 100 m from the monitored umbrella.

The measurement system consists of the following devices:

- 8 strain transducers HBM SLB-700A, to measure the longitudinal strain of the upslope flange of the HEB 120 beams, mounted on the internal side (T1–T8 in Fig. 4);
- 8 strain gauges HBM K-LY41-6/350 arranged in two full Wheatstone bridges, to measure the axial strain of the anchor plates;

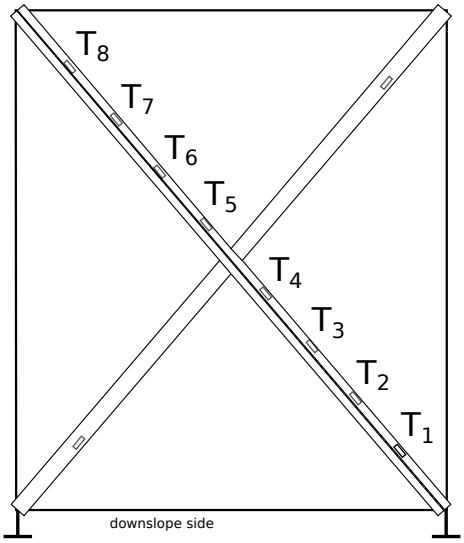

Figure 4: Position of the strain transducers (upslope view of the downslope side).

- 1 acquisition and control unit National Instruments CompactRIO, with 2 modules for strain gauges, placed in a watertight box, buried in the vicinity of the instrumented umbrella and connected to a solar-powered battery system through a 100 m cable, running in a protective duct fixed with steel braces to the ground.

All the measuring devices and their cabling had to be mounted on site, on a barrier already in place. The strain transducers, which have been bolted to the steel profiles of the chosen umbrella, are self contained and temperature compensated instruments. The anchor plates had been prepared in the laboratory by gluing and protecting the strain gauges and the wirings, and then installed on site substituting the original ones.

All the cables connecting the strain transducers to the acquisition and control unit run through watertight ducts, fixed to the structure or buried for protection against damage from impacts and snow gliding. The whole system drains a current of about 200 mA at 24 V.

Through the modules plugged into the acquisition and control unit, all the instruments are fed with a predetermined current, and voltage. For each instrument, the bridge unbalance voltage, which gives a measure proportional to the strain of the structure at that point, is recorded.

3.3 Measured data

The system is controlled by a software developed in the NI LabView environment, conceived to acquire the signals from the 8 strain transducers on the beams and the 2 strain gauge bridges on the anchor plates every 30 min and to store the measurements safely in daily files resident in the solid state drive of the data logger. In the first winter after installation, it was operational during the period from October 15, 2010, to April 26, 2011 (except on two consecutive days in late December), for a total of 190 days and 9120 values for each of the 10 instruments. Unfortunately, the strain transducer T4 and one of the two measuring bridges on the anchor plates did not function properly since the first day, and their measurements have been disregarded in all the analyses.

Notwithstanding the declared compensation of the instruments against temperature variations, the measurements show a clear, although small, daily oscillation, probably due to the transient

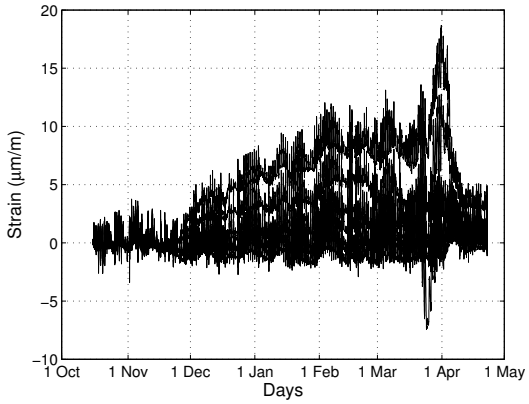

Figure 5: Strain measured by the transducers on the HEB beam every 30 min.

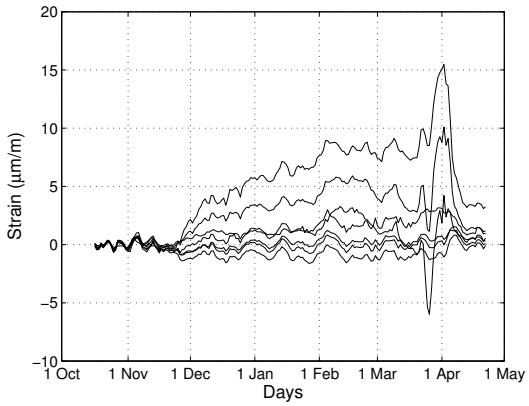

Figure 6: Daily averages of the strain measured by the transducers.

warming of the structure and the consequent difference of temperature between the transducer body and the beam (Fig. 5). To filter this effect, the daily average of the measurements has been calculated, obtaining smoother curves, as shown in Figure 6. It has to be remarked that, to account for the initial offset of the different instruments, due to small residual deformations induced by the installation procedure, the average of the first 3 week, period without snow cover at the site, has been subtracted from each series of measurements.

The height of snow has been estimated only by visual inspection, and is listed in Table 1.

As stated above, only one of the instrumented anchor plates worked properly during the monitoring period, giving acceptable results. The strain-history of the plate is presented in Fig. 7, with all the measured data, and in Fig. 8 with the daily-averaged values. These measurements have also been adjusted so that their average calculated on the first three weeks of recording is zero.

Table 1: Height of snow measured during the monitoring period.

Period	Date	Snow height (m)
—	15 October 2010	0.00 ± 0.00
A	20 January 2011	0.50 ± 0.10
B	4 March 2011	1.00 ± 0.10
—	26 April 2011	0.00 ± 0.00

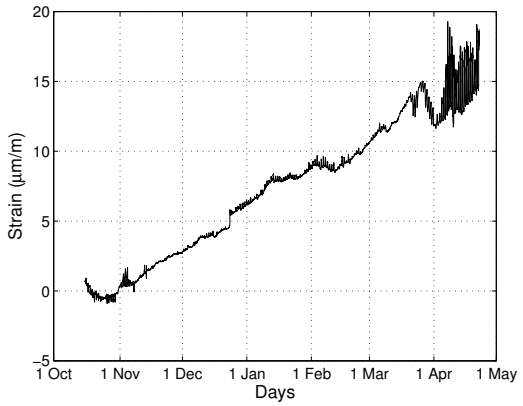

Figure 7: History of the strain of the anchor plate: raw data.

4 Interpretation of the measurements

4.1 Method

The transducers installed on the instrumented umbrella measure the strain of the structural elements; the evaluation of the pressure exerted by the snow on the retaining net requires an interpretative model correlating the two quantities. Hence, it is necessary to build a mathematical model of the loaded barrier that outputs the strain in the structure when subjected to a distribution of pressure representing the thrust of the snow.

After the development of a structural model that describes the statics of the structure, it is necessary to describe the pressure distribution. As detailed in the following, given the snow depth, the comparison between the strain values computed with the structural model and the corresponding measured strains gives information about the effectiveness of the model and the magnitude of forces.

4.2 Structural model

To accurately model the rigid beams and the flexible net panel that arrests the downward motion of the snow is a difficult task. Since the retaining structure is flexible, with imprecise loading conditions, the determination of its mechanical response would require the solution of a complex problem of interaction between the umbrella and the snowpack. Moreover, setting up a comprehensive model of this kind requires a knowledge of the mechanical behavior of snow that is beyond the scope of this work.

In order to obtain a simple idealization of the loads acting on the snow umbrella, it is assumed that, due to the obstruction to motion generated by the net panel, a linear distribution of surface

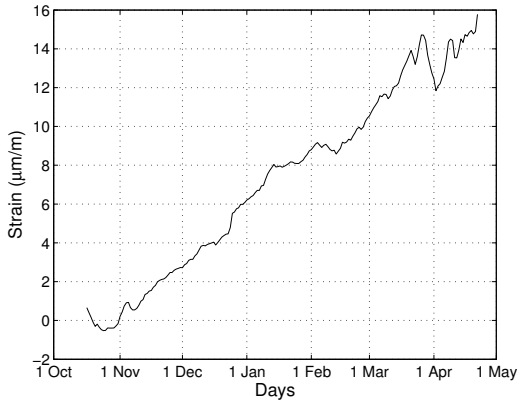

Figure 8: History of the strain of the anchor plate: daily averages.

forces arises, generally acting both in the normal and in the parallel direction (with respect to the net panel). To evaluate the load acting on the beams, the surface of the net is idealized as composed by 4 triangular zones (Z1–Z4 in Fig. 9) each one divided into narrow strips, parallel to the outer edges, fixed to two arms of the cross [9].

Keeping into account the height of the snow, the support reactions of each strip are calculated as for simply supported beams loaded by normal or tangential pressure components. The reactions so calculated are considered as the load acting on the cross beams, producing the strain to be compared with the measurements.

After determining the load on the cross beams, the reactions at the feet of the panel and at the anchor point can be determined, writing the usual equilibrium equations, considering also the actions of the cables, which can act only with tensile forces. The structural schematic is shown in Fig. 10. Referring to the figure, the snowpack, whose total vertical depth is h, is shaded in grey. The pressure values are denoted as p_r, at ground level, and p_m at a depth x below snow surface. The is hinged at the foundation and simply supported at the feet.

The strains at the positions of the transducers T1-T8 are calculated with the usual equations of structural mechanics.

As an example, the graph of Fig. 11 depicts the strain generated at the interior surface of the upslope beam flange, by a constant uniform pressure of 1.0 kPa, normal to the net panel and applied from ground level to 1.0 m. The origin of the diagram is at the foot of the beam.

The sharp peak corresponds to the position of the lower cable, which in this case is the active one. For this and all the results presented here, the width of the strips of the net panel used in calculating the load was 1/1 000 th of the beam length.

4.3 Evaluation of snow pressure

The evaluation of snow pressure presupposes that a pressure distribution and a reference pressure are set. Since the shape of the bending moment diagram in a linear elastic beam does not depend on the magnitude of the applied load, but only on its spatial distribution, first, the most correct pressure distribution has to be chosen. Then, the magnitude can determined by increasing or reducing the reference pressure, i.e. by scaling the pressure distribution but keeping its shape.

The first step is made by (i) assuming a pressure distribution, with a magnitude defined by an arbitrary reference value, p_r. (ii) This load is applied to the structural model of the snow

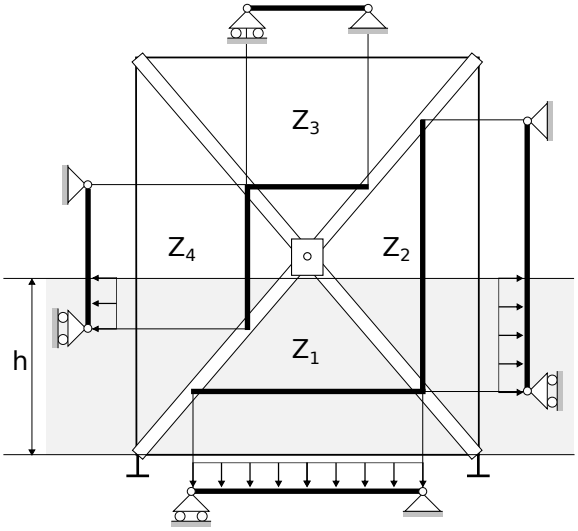

Figure 9: Scheme of the net panel as an assemblage of strips and evaluation of the load on the beams.

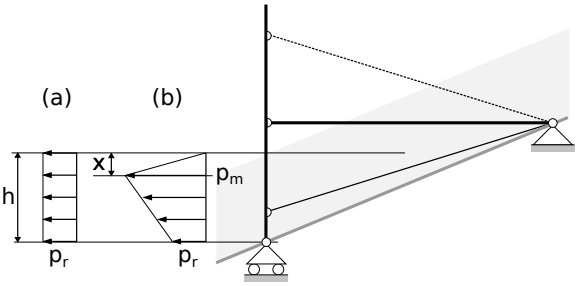

Figure 10: On left-hand side, two distributions of load on the snow supporting structure are shown: (a) uniform pressure and (b) bi-linear pressure. On the right-hand side the schematic of the structure model is represented.

umbrella, producing a bending moment in the cross beams. (iii) The strains in the structural elements are computed and plotted against the corresponding measured quantities. Since continuous measurements of snow height were not available, the strains used for the analysis of the device derives from the averages over two periods: (A) from 11 to 18 January and (B) from 24 February to 3 March. These values are listed in Table 2.

For correlation, the supposed pressure distribution may be a correct evaluation of the real one [3]. The magnitude of the load, q_r and q_m, is the product of the slope of the regression line, k, in the plane measured *vs* computed strains and the pressure value, p_r and p_m, respectively. In the structural of the snow umbrella model, the computed values of pressure refer to the forces perpendicular to the net panel.

As detailed in the following paragraphs, two different pressure distribution have been analyzed. The first one assumes a constant pressure through the depth of the snowpack, (diagram (a) in Fig. 10). The second one models a variable pressure distribution, which has been idealized with a bi-linear trend (diagram (b) in Fig. 10). Both pressure distributions refer to the total snow depth, h.

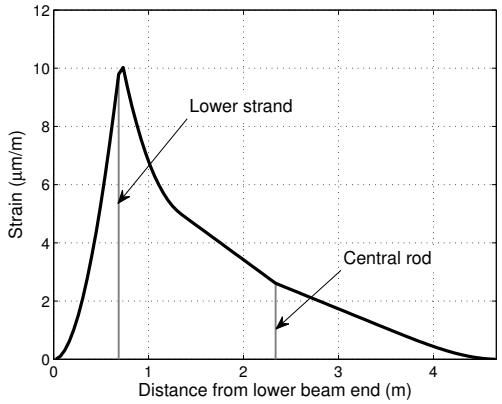

Figure 11: Longitudinal strain produced by a uniform unit pressure applied normally to the net panel in the range from 0 to 1.0 m.

Table 2: Mean values and standard deviations of the measured strains, in μm/m.

Strain	Period	
Tranducer	A - 20 Jan, 2011	B - 4 Mar, 2011
T1	1.09 ± 0.22	1.85 ± 0.50
T2	3.53 ± 0.46	4.85 ± 0.62
T3	6.46 ± 0.66	8.17 ± 0.48
T5	1.38 ± 0.49	1.85 ± 0.31
T6	0.33 ± 0.38	0.32 ± 0.20
T7	0.12 ± 0.39	-0.12 ± 0.25
T8	-0.65 ± 0.37	-1.14 ± 0.21
Plate	7.80 ± 0.37	10.21 ± 0.31

4.3.1 Uniform pressure distribution

In this case, a single parameter controls the behavior of the structural model, i.e. the reference pressure p_r. Plotting the measured values versus the corresponding computed strains, a certain linear correlation is found as shown in Fig. 12. Here the reference pressure is set at 1 kPa. The circles refer to 20 Jan data and the dashed black line represents their regression line, with slope 0.514. The crosses refer to 4 Jan data and the plain black line represents their regression line, with slope 0.927. As stated previously, the reference pressure has to be multiplied by the slope in order to get equal scales on both axes of the plot. The Pearson's correlation factors. ρ, and the p-values are reported in Table 3. Pearson's correlation factor, ρ, varies between -1 and +1, showing perfect (positive or negative) correlation at ± 1 and non-correlation at 0. The consistency of the correlation is further highlighted by the p-values, i.e., the probability that the calculated value of the correlation factors are due to an extreme situation in which the hypothesis of no correlation is true. If the p-value is smaller than 0.05, which is a value found to be adequate to represent a satisfactory level of significance, the null hypotheses are rejected [13] and, thus, a correlation is shown. In the case of constant pressure distribution, the p-values are smaller than 0.05 for the data measured in both the dates analyzed.

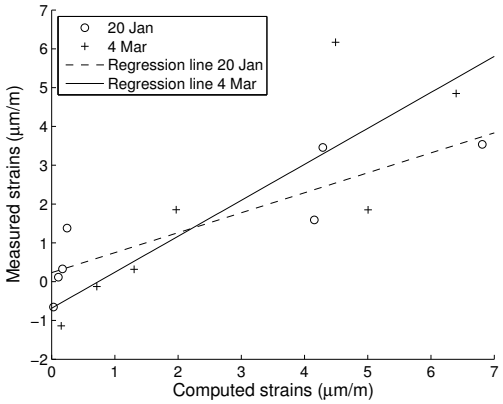

Figure 12: Uniform pressure distribution: measured strains versus computed strains in case of a reference pressure $p_r = 1\,\text{kPa}$.

Table 3: Uniform pressure distribution: statistical parameters of the correlation (Pearson's factors ρ and p-values)between the measured and computed strains.

Period	Date	Snow depth [m]	ρ	p-value
A	20 Jan, 2011	0.50	0.8802	0.0089
B	4 Mar, 2011	1.00	0.8378	0.0186

The value of the uniform pressure that best fits the measured data is obtained by multiplying the slope of the regression line and the reference pressure. In this first case the real pressures are 0.51 kPa for a snowpack depth of 0.50 m, and 0.93 kPa for a snowpack depth of 1.0 m.

4.3.2 Variable pressure distribution

A second analysis of the measured data assumes a pressure distribution which varies with depth. As shown in Fig. 10(b), the pressure distribution is supposed bilinear, with top pressure null. The distribution is governed by 3 parameters: p_r the reference pressure at bottom, $\xi = x/h$ the relative position of the turning point in the distribution, and $\eta = p_m/p_r$ the relative pressure at a distance x from the snow surface. The values of η and ξ define the shape of the pressure distribution. For example, $\eta = 1$ and $\xi = 0$ refer to a uniform distribution, $\eta = 0.5$ and $\xi = 0.5$ to a triangular distribution, and $\eta = 1$ and ξ variable to a trapezoidal pressure distribution.

The reference pressure, as seen in the previous section, acts only as a scale factor for the load distribution. In order to found the best fitting pressure distribution, for sake of simplicity and differently from the previous analysis shown in Fig. 12, p_r is now set equal to 1 Pa. Therefore, only two parameters governs the optimization problem. For a given pair of shape parameters $(\xi;\eta)$, Pearson's correlation factors, ρ_A and ρ_B (see Table 4), between computed and measured strains are evaluated and their minimum

$$\rho_{\xi,\eta} = \min\left(\rho_A;\rho_B\right) \tag{1}$$

is considered.

By varying the values of ξ in the range $(0;1)$ and η in the range $[0.01;1000]$, the best set is the one that maximizes the value of $\rho_{\xi,\eta}$. Figure 13 depicts the contours of $\rho_{\xi,\eta}$ as a function of its

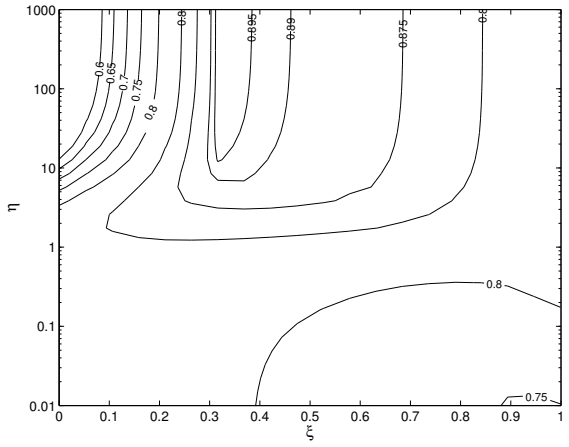

Figure 13: Variable pressure distribution: evaluation of the minimum correlation factor $\rho_{\xi,\eta}$ for each couple of shape parameters of the load distribution, $(\xi;\eta)$. The maximum occurs at $\xi \approx 0.32$ and η variable from 100 to 1000.

parameters. It can be noted that the maximum, slightly larger than 0.895, is defined for a set of points of the plot of Fig. 13.

The correlation factor is maximized at $\xi \approx 0.32$ and for η values varying from 100 to 1000. Apparently, it seems that the shape of the pressure distribution is highly affected by the ratio between the pressure at the turning point and the pressure at the base. Despite this ratio varies largely, the correlation is almost constant with high value. In order to assess the variability of the pressure distribution as a function of parameter η, the slope of the regression line, representing the multiplier of the pressure at the base p_r is computed for $\eta = [10, 1000]$. For both data sets, the best-fit pressure at the base is determined and, thus, the real maximum value q_m is defined. As can be seen in Fig. 14, where the values of q_m for various η are plotted, the maximum pressure is almost constant, independent of the value of the shape parameter η. This is explained by the fact that the pressures at the base, q_r, shown in the inner graph of Fig. 14, are very small if compared with their maximums and, thus, can be considered equal to zero. From this numerical evidence derives that the load distribution can be identified with a bi-triangular shape with apex at 0.30 times the height of the snowpack measured from its surface.

Figure 15 shows the correlation (Pearson's factors ρ and p-values) between computed and measured strains for a pressure distribution whose shape parameters ξ and η are 0.32 and 1000, respectively. The circles refer to 20 Jan data and the dashed black line represents their regression line, with slope 1.615. The crosses refer to 4 Jan data and the plain black line represents their regression line, with slope 3.517. The reference pressure has to be multiplied by the slope in order to get equal scales on both axes of the plot. Pearson's correlation factors, and the p-values corresponding to the rejection of the hypothesis of no correlation are reported in Table 4, for $\eta = 100$ and $\eta = 1000$; ξ is kept constant to 0.32.

4.4 Anchor reaction

The measurement of the strain of the anchor plates gives a direct evaluation of the total thrust on the structure. The strain, as can be seen in Fig. 8, presents a quite monotonic increase, and the maximum value is recorded at the very end of the period. It is remarkable that no elastic rebound appears after the melting of the snow cover, and an irreversible state of stress remains in

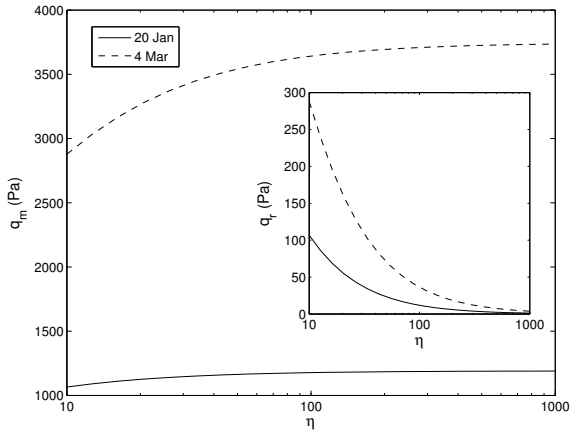

Figure 14: Variable pressure distribution: value of the maximum pressure, q_m, derived derived from various couples $(\xi;\eta)$ with fixed $\xi = 0.32$; η varies from 10 to 1000, in the range where the largest correlation is found. In the inner graph, the values of q_r, pressure at ground, are plotted.

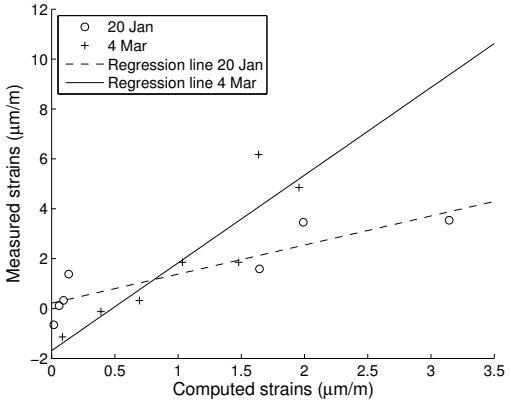

Figure 15: Variable pressure distribution: measured strains versus computed strains in case of a reference pressure, $p_r = 1\,\mathrm{Pa}$.

Table 4: Statistical parameters of the correlation between the measured and computed strains.

			$\eta = 100$		$\eta = 1000$	
Period	Date	Snow depth [m]	ρ	p-value	ρ	p-value
A	20 Jan, 2011	0.50	0.8967	0.0062	0.8971	0.0062
B	4 Mar, 2011	1.00	0.9063	0.0049	0.9070	0.0048

Table 5: Total forces in the anchor rod.

Period	Date	Snow depth (m)	F (kN)
A	20 Jan, 2011	0.50	4.00 ± 0.19
B	4 Mar, 2011	1.00	5.23 ± 0.16

the structure even after the snow load removal. This fact can be explained by introducing into in the structural model a cause of energy dissipation as, for example, friction.

It can be argued that, in the course of the winter season, the feet of the structure, realized with steel plates resting on a horizontal base excavated on the slope, could slide downslope under increasing snow thrust, able to exceed the friction resistance. When the load decreases, as happened several times during the monitored period, only minor recovery of the deformation of the anchor plates is observed, which permits to conclude that the foot acts as a friction slider, i.e. it would require an upward thrust to return to its original position.

Because of the failure of one of the strain gauge bridges, the maximum load on the foundation could only be estimated by assuming that the two plates would have suffered the same strain. For a given measured strain ε, the total force, F, on the anchor rod is given by

$$F = 2\frac{EA}{\kappa}\varepsilon \tag{2}$$

where $E = 210\,\text{GPa}$ is Young's modulus, $A = 1000\,\text{mm}^2$ is the cross-sectional area of the plate, and $\kappa = 0.82$ is a concentration factor, calculated with a plane stress finite element model of the plate, at the point where the strain is measured. Table 5 lists the values of the forces in the anchor rod found from Eq.(2).

The difference between this force and the snow thrust is probably due to the horizontal frictional force arising at the interface between the steel plates of the feet and the soil.

5 Conclusions

A preliminary analysis of the measurements of the strains induced by snow loading on a new retaining structure has been presented. As shown by the measured strains, the cross beams of the snow umbrella are able to support the snow pressure on the flexible net. The technique set up for comparing the results of the model and the measured values on the strain gauges considers the correlation between the two sets of data. This technique is shown to be effective, since the correlation factor is independent of the value of the pressure, but dependent on the shape of the distribution. The slope of the linear regression line plays an important role in the estimation of the magnitude of the snow thrust (see Fig. 12 and Fig. 15).

Two different pressure distributions have been assumed. In both cases, Pearson's correlation coefficients are found greater than 0.50, showing some sort of correlation between the measured and the computed strains (see Tables 3 and 4). The consistency of the correlation is further highlighted by the p-value, a statistical parameter used for testing the hypothesis of no correlation against the alternative that there is a nonzero correlation. Under a significance level of 0.05, the null hypotheses are rejected, thus a correlation is shown.

The overall results of the analysis herein proposed are reported in Table 6. In the case of uniform pressure distribution, q_r is the magnitude of the constant distribution and F_U is the resultant force per meter width. In the case of variable pressure distribution, q_m is the maximum pressure, corresponding to the turning point of Fig. 10(b) and F_V is the resultant force per meter width

Table 6: Comparison between the results of the analysis for two different pressure distributions.

Period	Date	q_r	F_U	q_m	F_V	F_R
A	20 Jan, 2011	0.51 kPa	0.25 kN/m	1.88 kPa	0.47 kN/m	1.29 kN/m
B	4 Mar, 2011	0.92 kPa	0.92 kN/m	3.73 kPa	1.86 kN/m	1.69 kN/m

computed supposing that the distribution assumes null values at its ends. F_R is the resultant force per meter width computed dividing the total force at the anchor rod, see Table 5, by the width of the barrier (3.1 m).

As a first consideration, the variable distribution produces resultant forces larger than those predicted by the uniform distribution.

In order to assess the effectiveness of the model, the resultant forces computed from this preliminary investigation have been compared with the corresponding values found in the Swiss Guidelines [5]. Referring to a snow depth equal to 0.50 m, the guidelines suggest a force parallel to the slope of about 0.32 kN per meter width ($\rho_s = 300\,\mathrm{kg\ m^{-1}}$, $\psi = 30°$, $K = 0.658$, $N = 1.3$). In the case of snow depth equal to 1.00 m, the guidelines suggest a force parallel to the slope of about 1.28 kN per meter width ($\rho_s = 300\,\mathrm{kg\ m^{-1}}$, $\psi = 30°$, $K = 0.658$, $N = 1.3$). Projecting the aforementioned terms on the direction normal to the net panel, one gets 0.37 kN/m and 1.47 kN/m. These values are compatible with the results of the investigation: in both cases the value found in the guidelines is in-between the estimations from the measured data, as shown in Table 6. It is necessary to specify that the values found in the guidelines depend upon the density of the snow, which is an unmeasured parameter in our analysis.

Following the preliminary analysis presented in the paper, two main conclusions can be drawn.

i. From the structural point of view, the state of stress and strain measured in the rigid parts of the barrier are well below the elastic limit of steel. This could be perceived as an oversizing of the structure. Although this conclusion cannot be generalized, keeping in mind the fact that winter 2010/2011 was characterized by low snow precipitation and reduced snowpack depths, lower that 1/3 of the total height of the barrier. In this sense, this result confirms what found by Peila et al. [10] on the loads acting on the cables of the structure. Anyway, their observations were limited to one winter season, which cannot be necessarily representative of the limit situation that the structure may suffer.

ii. From the point of view of snow-mechanics, the methodology presented in the paper allowed us to formulate a rough estimate of the pressure on the barrier. This method, which couples structural mechanics and observations, although indirect, is effective even if the number of measured parameters is reduced. For example, in our analysis, only the strains in the cross beam and snow heights were measured.

The technique proposed in the paper is flexible and can be extended to other similar configurations of measuring devices. Increasing the number of strain transducers together with a continuous recording of snow height in the neighborhood would lead to a more reliable estimate of the snow pressure on similar retaining structures.

6 Acknowledgements

The financial support provided by Regione Autonoma Valle d'Aosta, Assessorato opere pubbliche, difesa del suolo e edilizia residenziale pubblica, Direzione Assetto idrogeologico dei bacini montani

in the framework of the Interreg Project RISK-NAT Italia/Francia (Alpi 2007-2013) is gratefully acknowledged. The authors would like to thank Dr E. Bovet, Prof B. Chiaia, Dr B. Frigo and Dr M. Maggioni for their contributions in the researches conduced onsite. Thanks also to Betonform for supplying the anchor plates later instrumented and installed in situ.

References

[1] V. De Biagi, B. Chiaia, and B. Frigo. Structural back-analysis of avalanche impact on buildings. submitted to CRST, 2012.

[2] V. De Biagi, B. Chiaia, and B. Frigo. Vulnerability of buildings against avalanche hazard. In T. Fukuhara and T. Takahashi, editors, *Snow Engineering VII: Proceedings of the Seventh International Conference on Snow Engineering, 6-8 June 2012, Fukui, Japan*, pages 53–68, 2012.

[3] A.L. Edwards. *An Introduction to Linear Regression and Correlation*. W. H. Freeman, San Francisco, CA, 1976.

[4] R. Haefeli. Vorschläge zur konstruktion und berechnung von netzwerken. Technical report, Eidgenössisches Institut für Schnee- und Lawinenforschung, Davos, 1954. Externer Bericht Nr. 2112.

[5] S. Margreth. Defense structures in avalanche starting zones. technical guideline as an aid to enforcement. *Environment in Practice. FOEN, SLF, Bern and Davos*, 2007.

[6] D. McClung and P. Schaerer. *The avalanche handbook*. The Mountaineers Books, 2006.

[7] F. Nicot. From constitutive modelling of a snow cover to the design of flexible protective structures. part i–mechanical modelling. *International Journal of Solids and Structures*, 41(11–12):3317–3337, 2004.

[8] F. Nicot, M. Gay, and J.M. Tacnet. Interaction between a snow mantel and a flexible structure: a new method to design avalanche nets. *Cold Regions Science and Technology*, 34(2):67–84, 2002.

[9] G. Olivero. Opere di difesa attiva dalle valanghe di neve: studio teorico e sperimentale di una struttura a ombrello, 2011. Master thesis, Politecnico di Torino, in Italian.

[10] D. Peila, C. Oggeri, and V. Betti. Studio sperimentale del comportamento di un nuovo modello di opera stabilizzatrice del manto nevoso. *GEAM, Geoingegneria ambientale e mineraria*, XLII(1):93–99, 2005.

[11] E. Rainer, L. Rammer, and T. Wiatr. Snow loads on defensive snow net systems. In T. Jóhannesson, G. Eiríksson, E. Hestnes, and J. Gunnarsson, editors, *International Symposium on Mitigative Measures against Snow Avalanches, Egilsstadhir, Iceland*, pages 40–47, 2008.

[12] V. Segor, C. Vicari, F. Saravalle, and R. Di Bella. A new system of rapidly installed avalanche barriers. In *Proceedings of the International Snow Science Workshop 2010, Squaw Valley, CA*, 2010.

[13] Thomas Sellke, M. J Bayarri, and James O Berger. Calibration of ρ values for testing precise null hypotheses. *The American Statistician*, 55(1):62–71, 2001.

[14] US National Research Council. *Snow avalanche hazards and mitigation in the United States*. National Academies Press, 1990. Panel on Snow Avalanches and National Research Council (US). Committee on Ground Failure Hazards Mitigation Research.